Towards an intermediate water wave model of vocal fold vibration: Evidence from vocal-fold dynamic sonography

*Chen-Gia Tsai[*1], Tzu-Yu Hsiao[*1], Yio-Wha Shau[*2], and Jeng-Horng Chen[*3]*

[*1)]Department of Otolaryngology, National Taiwan University Hospital, College of Medicine, National Taiwan University, Taipei, Taiwan
[*2)]Institute of Applied Mechanics, National Taiwan University, Taipei, Taiwan
[*3)]Department of Systems and Naval Mechatronic Engineering, National Cheng Kung University, Tainan, Taiwan
tsaichengia@ntu.edu.tw

Abstract

A simplified water wave model was developed for predicting the global vibration of human vocal folds. As the depth of the liquids in the lamina propria is 1/2–1/20 of the wavelength, they were analogized to intermediate waters. The water wave model predicted elliptic orbits of the tissue particles with the major axis parallel to the surface, and these ellipses flattened with depth. This vibration behavior was verified by ultrasound imaging of the vocal fold during modal phonation. The possible mechanical roles of different layers of the vocal fold were discussed in the light of the water wave model. The epithelium may provide the restoring forces of the water waves, whereas the vocal ligament may serve as a wave damper, an impedance matcher, and an energy saver. The liquids in Reinke's space play a key role in the conversion between the circular motion on the vocal-fold surface to the tangential motion in the vocal ligament. This water wave model may be viewed as a start point of the poroelasticity model of vocal fold vibration.

1. Introduction

The highly pliable property of Reinke's space is unique to human tissues. This space comprises loose fibers and interstitial proteins with a high water content. When a knife cuts a leak on the epithelium, gel-like materials issue from Reinke's space. Previous studies have emphasized the roles of this strongly hydrated gel in tissue viscosity, shock absorption, and space filling (for a recent review, see Ward et al. 2002). It has been shown that the vocal fold hydration level affects vocal fold vibration in a dramatic manner (e.g., Chan and Tayama 2002).

From a viewpoint of biomechanics, the lamina propria of the vocal fold can be regarded as a multilayered liquid-saturated porous medium. A formal approach to physical modeling may be Biot's (1941, 1956) poroelasticity theory, which accounts for wave propagation in a two-component medium composed of a porous solid frame and a pore fluid. Biot's equations are derived from (1) equations of linear elasticity for the solid frame, (2) Navier-Stokes equations for the viscous fluid, and (3) Darcy's law for the interaction between the fluid and the solid frame due to their relative motion. Poroelasticity has a wide range of applications to the study of biological tissues, such as bones, cartilages, skins, lungs, arterial or myocardial tissues.

In the present study, we assume that the fibers in Reinke's space are fine and loosely folded, and the wave amplitude in the vocal ligament is small, so that the liquid-like nature dominates vocal fold vibration. In this approximation, we used a water wave theory (Airy 1841) to predict the global vibration of the vocal fold, while the damping effect of the fibrous frames in the lamina propria is discussed as a correction. Our single-phase model may be viewed as a start point of the poroelasticity model of vocal fold vibration.

In physical oceanography, water waves are classified by the ratio of the water depth H to the wavelength λ as deep ($H/\lambda > 1/2$), intermediate ($1/2 > H/\lambda > 1/20$), or shallow ($1/20 > H/\lambda$). For vocal fold vibration, the total thickness of the epithelium and the lamina propria is approximately 3–5 mm, and λ is approximately 11 mm for male modal phonation (for phonation frequency f = 90–160 Hz, mucosal velocity c_m = 1–2 m/s. Tsai et al. in preparation). Although the bottom of the water layer in the vocal fold is not well defined, it is evident that $1/2 > H/\lambda > 1/20$, and its dynamics may be analogous to intermediate water waves. Particles in intermediate water waves follow elliptic orbits with the major axis parallel to the bottom. These ellipses flatten with depth, and particles near the bottom are primarily involved in tangential motion (Fig. 1). This vibration behavior is inconsistent with the assumption of lateral motion of the vocal-fold body in previous models (Hirano 1974, Story and Titze 1995, Titze 1988, Liljencrants 1991). We suggest that the ratio of tangential-to-normal displacements of the body layer is a criterion for distinguishing between the previous low dimensional models and the intermediate water wave model of vocal fold vibration.

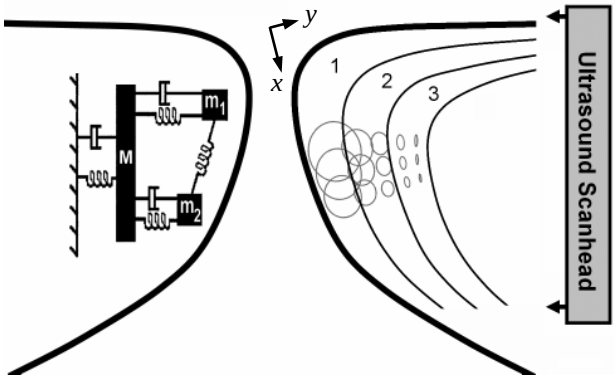

Figure 1. Comparison of the three-mass model (left) and the intermediate water wave model (right). The gray ellipses represent the orbits of tissue particles (clockwise motion) in the three layers of the lamina propria. Whereas the three-mass model assumes lateral motion of the body layer (M), the water wave model predicts dominant vertical motion of the deep lamina propria.

Measuring the body layer motion is more challenging than measuring the cover layer motion, because the body layer is inaccessible. Here we present a methodology for the noninvasive visualization of vocal-fold body motion using medical ultrasound. Traditionally, lack of interest in ultrasound

imaging of the vibrating vocal fold is partly due to its low frame rate. In the present study, the subject tuned the singing pitch *f* to be close to an integer multiple of the ultrasound frame rate f_s, and slowly-traveling, low-frequency waves of the vocal fold appeared in the 2D sonography. This technique shares some features with the low-frame-rate laryngoscopy. The sonographic data support the intermediate water wave model.

2. Theory

In the simplified water wave model, the liquids in Reinke's space are assumed to be homogeneous, incompressible, inviscid, and two dimensional. Like water waves, the flow in Reinke's space is a potential flow, with the velocity potential governed by Laplace's equation: $\nabla^2\Phi(x,y)=0$.

Next, we compare the boundary conditions of water waves and the liquids in the lamina propria. The first boundary condition of water waves is the *kinematic condition*, which states that a parcel of fluid at the surface remains at the surface. Obviously, this condition is satisfied at the liquid-epithelium interface during vocal fold vibration. The second boundary condition of water waves is the *dynamic condition*: the pressure on the surface equals the atmospheric pressure p_a. This condition can be expressed by the Bernoulli equation:

$$\frac{\partial\Phi(x,w)}{\partial t}+\frac{p(x,w)}{\rho_w}+\frac{1}{2}\left|\nabla\Phi(x,w)\right|^2+gw=\frac{p_a}{\rho_w}, \quad (1)$$

where $p(x,y)$ is the liquid pressure, ρ_w is the liquid density, g is the acceleration due to gravity, and w is the deformation of the water surface.

A major difference between mucosal waves and water waves is the restoring force: whereas gravity provides the restoring force of a water wave, the restoring forces of liquid motion in Reinke's space are presumably provided by the tensioned epithelium. We assume that the epithelium is composed of parallel strings aligned in the anterior-posterior direction (*z*-direction in Fig.1), with no coupling between adjacent strings. Each string has the shape of a hyperbola when subject to a deformation w:

$$w(x,z)=\left(1-\frac{4z^2}{l_e^{\,2}}\right)w(x,0), \quad (2)$$

where l_e is the epithelium length, and the $z = 0$ plane is located at the middle-point of the vibrating portion of the vocal fold. This deformation of the epithelium produces a pressure on the water surface p_e:

$$p_e=T_e\tau\frac{d^2w}{dz^2}=-\frac{8T_e\tau}{l_e^{\,2}}w(x,0)=-\frac{8T_e\tau}{l_e^{\,2}-4z^2}w(x,z), \quad (3)$$

where T_e is the tensile stress on the epithelium and τ is its thickness. The dynamic condition for the liquids in Reinke's space becomes

$$\frac{\partial\Phi(x,w)}{\partial t}+\frac{p(x,w)}{\rho_w}+\frac{1}{2}\left|\nabla\Phi(x,w)\right|^2=\frac{1}{\rho_w}\left(p_a+p_e\right)=\frac{1}{\rho_w}\left(p_a-\frac{8T_e\tau}{l_e^{\,2}-4z^2}w(x,z)\right). \quad (4)$$

Eqs. (1) and (4) become identical if we define the "equivalent gravity acceleration" of mucosal waves as

$$g=\frac{8T_e\tau}{\rho_w\left(l_e^{\,2}-4z^2\right)}. \quad (5)$$

Although there is little evidence that the epithelium provides restoring forces, a recent study showed an intertwined network arrangement immediately below the epithelium (Madruga de Melo et al. 2003). The authors suggested that this basket-like configuration explained how the epithelium was able to stretch even though it contained nonstretchable fibers.

The last boundary condition of water waves is that there is no flow through the bottom. This condition is satisfied if we assume a rigid, impermeable bottom in the vocalis muscle.

A linear water wave theory states that the lengths of the major and minor axes of the elliptic orbit of water particle are

$$A(y)=w_0\frac{\cosh\left[k(H-y)\right]}{\sinh(kH)}, \quad (6)$$

$$B(y)=w_0\frac{\sinh\left[k(H-y)\right]}{\sinh(kH)}, \quad (7)$$

respectively, where y is the depth of the particle, k is the wave number, and w_0 is the wave amplitude on the surface.

3. Experiment

3.1. Methods

The orbits of tissue particles in the vocal fold were estimated from dynamic sonography. One of the authors (C.G. Tsai), a healthy man aged 35 years without voice disorders, was the subject of this study. A standard medical high-resolution ultrasound scanner (HDI-5000, ATL, Bothell, WA) with a linear-array transducer (CL10-5 25 mm, ATL) was used to record 2D sonography. The scanhead was placed in the coronal plane at the midline of the thyroid cartilage lamina on the right side during sustained loud modal phonation (Fig. 1).

3.2. Results

Dynamic 2D sonography of the vocal fold was recorded during steady phonation with *f* in the range of 116–118 Hz and f_s = 38 Hz. Since $f = 3f_s + q$ with $2 < q < 4$ Hz, the vibration frequency evident from dynamic sonography lied between 2 and 4 Hz. Similar to the stroboscopic implementation, performing vocal-fold dynamic sonography over a cycle allows for the estimation of the average vibratory pattern over several successive cycles of the actual vocal fold vibration. 90 images over 6 cycles of the dynamic sonography were recorded. Since the 72nd and 90th images appeared identical, we concluded that 18 images were recorded over the last visualized cycle, and $f = 3f_s + (f_s/18) = 116.1$ Hz. We performed speckle tracking on images 72–90 manually. Preliminary results shown in Fig. 2 accord well with the vibration pattern of an intermediate water wave that the orbits of the tissue particles were approximately elliptic, and these ellipses flatten with depth.

Most of the particle orbits in Fig. 2 have major axes with the same orientation. We thus set the *x*-axis parallel to this orientation. Because the vocal fold is curved and the water layer has a complex geometry, the water surface and the "water bottom" in the body layer are not parallel. In the simplified water wave model, however, the *x*-axis was

expected to represent the average orientation of the water layer. The lengths of the major and minor axes of the orbits were plotted in Fig. 3, with a comparison to the theoretical curves based on Eqs. (6) and (7). The water depth H was estimated as the distance between the air-mucosa interface and the location where the vibration of the vocal-fold body vanished. Estimation of the mucosal wave velocity c_m = 1.4 m/sec was based on the experiment by Tsai et al. (in preparation). The ratio H/λ = 0.41 lies in the range of intermediate waters.

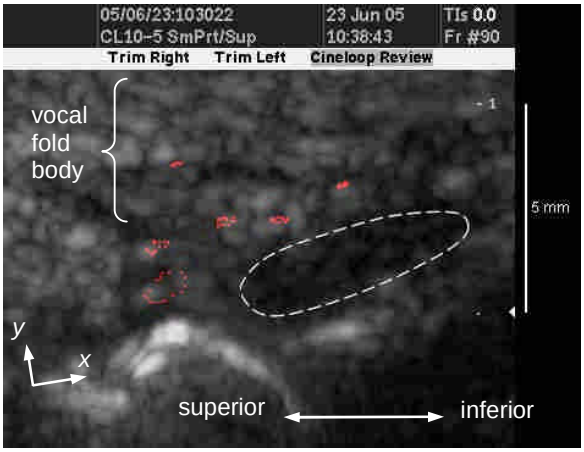

Figure 2: Ultrasound imaging of the right vocal fold during phonation. The white curve indicates the air-mucosa interface. The relatively dark region bounded by the dashed curve is Reinke's space, which mainly comprises hypoechoic liquids. The red dots represent the particle orbits. This movie is available at http://jia.yogimont.net/vf/icvpb.html

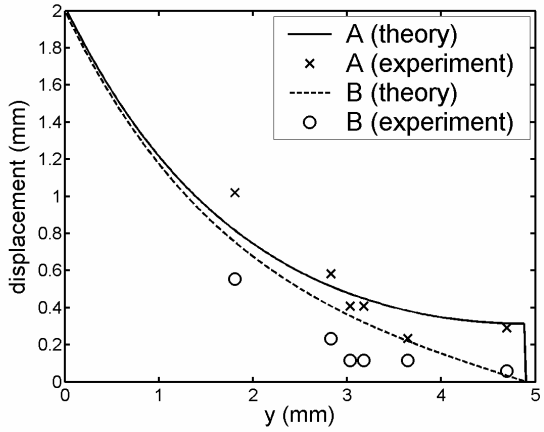

Figure 3: Experimental data of A(y) and B(y) compared to the theoretical curves based on Eqs. (6) and (7). H = 4.9 mm, f = 116.1 Hz, c_m = 1.4 m/sec, and w_0 = 2 mm.

4. Discussion

Particle orbits in the vocal-fold body were estimated from sonographic data obtained during modal phonation. Although the imaging quality was only moderate, it was evident that the particle motion was primarily tangential in the body layer. This result invalidates the assumption of some previous models that the vibration of the body layer is primarily lateral (Hirano 1974, Story and Titze 1995, Titze 1988, Liljencrants 1991), and supports the intermediate water wave model.

Several corrections should be added to this water wave model, such as (1) a three-dimensional flow, (2) a nonlinear flow due to large-amplitude vibration, (3) the viscous hysteretic response of the flow, (4) the nonlinear viscoelastic properties of the epithelium, (5) vocal fold collision, (6) the complex geometry of the water layer, and (7) the fibers in the lamina propria. The present study addresses only the last correction.

The fibers in the lamina propria have important effects on mucosal waves. First, the presence of loose fibers in Reinke's space may considerably increases the flow viscosity. Second, the lamina propria is inhomogeneous due to the *transition zone* between Reinke's space and the vocalis muscle; that is, the vocal ligament. The vocal ligament is presumably forced by the liquids in Reinke's space to also vibrate. Fine collagen fibers (type III) passing through Reinke's space, the vocal ligament, and the vocalis muscle (Madruga de Melo et al. 2003) may reinforce the cover-body coupling in the vocal fold through liquid-fiber interactions.

The water wave model of vocal fold vibration may provide insight into the mechanical roles of the vocal ligament. First, the elasticity of the vocal ligament might be responsible for attenuating the water wave near the bottom. In oceanography, friction with the seabed increases as waves approach intermediate/shallow water, and sometimes leads to problems of erosion and sedimentation, because water particles move forth and back at the bottom. In the vocal fold, the displacement of tissue particles may attenuate rapidly in the tensioned vocal ligament. In the other word, the vocal ligament may serve to match the impedances of Reinke's space and the vocalis muscle, thereby minimizing viscous losses due to velocity differences in the body layer. For loud phonation, this effect may be important for preventing tissue damage. In the comparison between the experiment data and theoretical curves (Fig. 3), however, the measured values of $A(y)$ and $B(y)$ in the vocal ligament (y = 3–4 mm) are only slightly smaller than theoretical curves. We suggest that the wave-damping effect of the vocal ligament may become significant when its tension is high, e.g., during high-pitched modal phonation.

Another role of the vocal ligament may be as an energy-saving mechanism. Whereas intermediate/shallow water waves lose energy through friction at the bottom, the strings in the vocal ligament (aligned in the z-direction in Fig.1) are able to convert a portion of kinetic energy into potential energy when displaced from their equilibrium positions. While these strings move to their equilibrium positions, they accelerate the liquids in Reinke's space, and thereby supply energy to water waves. This effect may improve the efficiency of loud vocalization. It is interesting to note that energy-saving springs can be found in numerous oscillation systems in animals, such as legs of mammals, insect flight, and dolphin/jellyfish/scallop swimming (for a recent review, see Alexander 2003).

The water wave model may shed new light on the function of the incompressible liquids in Reinke's space. Motion of the epithelium induces the liquid motion in Reinke's space and, since this layer is thin, the stiff wall of the vocalis muscle stops the impinging liquid and deflects the flow in the tangential direction. The liquid-like nature of Reinke's space might be responsible for the conversion between the circular motion on the surface to the tangential motion in the vocal ligament. A comparison between the water wave model and a solid finite-element model (Alipour et al. 2000) may highlight the importance of the liquids in Reinke's space. The lateral displacements on the inferior-medial surface predicted by that finite-element model were small, and the predicted particle orbits were more flattened than those measured experimentally (Baer 1975, Saito et al. 1985, Berry et al. 2001). This discrepancy may stem from the liquid-like nature of Reinke's space. It is interesting to note that the vibration behavior of the

lips of brass players (Yoshikawa and Moto 2003) shared some common features with the solid finite-element model of the vocal fold.

Lateral motion of the vocal fold plays a key role in absorbing the kinetic energy from the airflow, and therefore determines the vocal efficiency. We suggest that the liquid-like nature of Reinke's space is essential to produce significant lateral motion on the inferior-medial surface of the vocal fold.

5. Conclusions

This paper contributes experimental data on the ultrasonic visualization of vocal fold vibration, and presents a simplified water wave model based on these data. Owing to the involvement of nonlinear effects during large-amplitude vocal fold vibration and fiber distribution in the lamina propria, this model is still in its infant phase. At the present stage, we propose the possible mechanical functions of different layers of the vocal fold. Whereas the contributions of the epithelium and Reinke's space to the mechanical properties of the vocal fold have been seldom distinguished (e.g., Zhang et al. 2006), we treat the epithelium as a tensioned membrane that provides the restoring forces of the water waves in Reinke's space. Whereas the vocal ligament has been modeled as a string vibrating in the lateral direction, we suggest that its motion is primarily vertical, and it serves as a wave damper, an impedance matcher, and an energy saver. To model the interactions between the liquids and fibrous frame in the lamina propria, the dynamics of sea waves on a porous seabed may be relevant (e.g., Jeng et al. 2003). Numerical research on vocal fold vibration may use a biphasic finite-element method (e.g., Spilker and Maxian 1990). Furthermore, the approach and techniques of microrheology may help understand the viscoelastic and flow properties of the lamina propria at the micrometer length scale (e.g., Scheffold et al. 2004).

Medical ultrasound offers an unusual opportunity to visualize vocal fold vibration *in vivo*. Despite its limited temporal and spatial resolutions, there is growing interest in the ultrasound assessment of vocal fold function (e.g., Shau et al. 2001, Hsiao et al. 2002, Tsai et al. submitted). We are currently gathering ultrasonic imaging data to estimate the propagation velocities of mucosal waves and body waves (Tsai et al. in preparation), hoping to implement a more realistic vocal fold model.

6. References

Airy, G. B. (1841). "Tides and waves," in *Encyclopaedia Metropolitana* (1817–1845), *Mixed Sciences*, Vol. 3, edited by H. J. Rose, et al.

Alexander, R. M. (2003). "Functions of elastomeric proteins in animals," in *Elastomeric proteins: structures, biomechanical properties, and biological roles*, edited by P. R. Shewry, A. S. Tatham, and A. J. Bailey (Cambridge University Press), pp. 1–14.

Alipour, F., Berry, D. A., and Titze, I. R. (2000). "A finite element model of vocal fold vibration," J. Acoust. Soc. Am. 108, 3003–3012.

Berry, D. A., Montequin, D. W., and Tayama, N. (2001). "High-speed digital imaging of the medial surface of the vocal folds," J. Acoust. Soc. Am. 110, 2539–2547.

Biot, M. A. (1941). "General theory of three dimensional consolidation," Journal of Applied Physics 12, 155–164.

Biot, M. A. (1956). "Theory of propagation of elastic waves in a fluid-saturated porous solid, Part I: Low frequency range," J. Acoust. Soc. Am. 28, 168–177.

Chan, R. W., and Tayama, N. (2002). "Biomechanical effects of hydration in vocal fold tissues," Otolaryngol Head Neck Surg. 126(5), 528–537.

Chiba, T., and Kajiyama, M. (1958). "The vowel: its nature and structure," Phonetic Society of Japan, Tokyo.

Dean, R. and Dalrymple, R. A. (1991). *Water wave mechanics for engineers and scientists* (World Scientific, Singapore).

Hirano, M. (1974). "Morphological structure of the vocal cord as a vibrator and its variations," Folia Phoniatr. 26(2), 89–94.

Hsiao, T. Y., Wang, C. L., Chen, C. N., Hsieh, F. J., and Shau, Y. W. (2002). "Elasticity of human vocal folds measured *in vivo* using color Doppler imaging," Ultrasound Med. Biol. 28, 1145–1152.

Jeng, D. S., Lin, M., and Cha, D. H. (2003). "Revisit of poroelastic models for wave damping in a porous seabed: Comparison of existing models," Engineering Mechanics'03, ASCE, July 16–18, 2003, Seattle, USA.

Liljencrants, J. (1991). "A translating and rotating mass model of the vocal folds," STL Q. Progr. Stat. Rep., 1, Speech Transmission Laboratory, KTH, Stockholm, Sweden.

Madruga de Melo, E. C., Lemos, M., Aragao Ximenes Filho, J., Sennes, L. U., Nascimento Saldiva, P. H., and Tsuji, D. H. (2003). "Distribution of collagen in the lamina propria of the human vocal fold," Laryngoscope 113(12), 2187–2191.

Saito, S., Fukuda, H., Kitahira, S., Isogai, Y., Tsuzuki, T., Muta, H., Takyama, E., Fujika, T., Kokawa, N., and Makino, K. (1985). "Pellet tracking in the vocal fold while phonating: experimental study using canine larynges with muscle activity," in *Vocal Fold Physiology*, edited by I. R. Titze and R. C. Scherer (Denver Center for the Performing Arts, Denver, CO), pp. 169–182.

Scheffold, F., Romer, S., Cardinaux, F., Bissig, H., Stradner, A., Rojas-Ochoa, L. F., Trappe, V., Urban, C., Skipetrov, S. E., Cipelletti, L., and Schurtenberger, P. (2004). "New trends in optical microrheology of complex fluids and gels," Prog. Colloid Polym. Sci. 123, 141−146.

Shau, Y. W., Wang, C. L., Hsieh, F. J., and Hsiao, T. Y. (2001). "Noninvasive assessment of vocal fold mucosal wave velocity using color Doppler imaging," Ultrasound Med. Biol. 27, 1451–1460.

Spilker, R. L., and Maxian, T. A. (1990). "A mixed-penalty finite element formulation of the linear biphasic theory for soft tissues," Int. J. Num. Meth. in Engng. 30, 1063–1082.

Story, B. H., and Titze, I. R. (1995). "Voice simulation with a body-cover model of the vocal folds," J. Acoust. Soc. Am. 97, 1249–1260.

Titze, I. R. (1988). "The physics of small amplitude oscillation of the vocal folds," J. Acoust. Soc. Am. 83, 1536–1552.

Tsai, C. G., Shau, Y. W., and Hsiao, T. Y. "Laryngeal mechanisms during human 4 kHz vocalization studied with CT, videostroboscopy, and color Doppler Imaging" (submitted).

Tsai, C. G., Hsiao, T. Y., and Shau, Y. W. "Measurements of wave velocity in the vocal-fold cover/body layers during phonation using dynamic sonography" (in preparation).

Ward, P. D., Thibeault, S. L., and Gray, S. D. (2002). "Hyaluronic acid: its role in voice," J Voice. 16(3), 303–309.

Yoshikawa, S., and Moto, Y. (2003). "Lip-wave generation in horn players and the estimation of lip-tissue elasticity," Acustica/Acta Acustica 89, 145–162.

Zhang, K., Siegmund, T., and Chan, R. W. (2006). "A constitutive model of the human vocal fold cover for fundamental frequency regulation," J Acoust Soc Am. 119(2), 1050–1062.